Arabian Journal of Chemistry (2020) 13, 8920–8934

King Saud University

Arabian Journal of Chemistry

www.ksu.edu.sa
www.sciencedirect.com

ORIGINAL ARTICLE

The behavior of natural biomass materials as drug carriers in releasing loaded Gentamicin sulphate

Ashraf Bayoumi [a], Marwa T. Sarg [a], Tamer Y.A. Fahmy [b], Noha F. Mohamed [b], Waleed K. El-Zawawy [b,*]

[a] *Organic Chemistry Department, Faculty of Pharmacy, Al-Azhar University, Cairo, Egypt*
[b] *Cellulose and Paper Department, National Research Centre, 33 El-Bohouth St. (former El-Tahrir St.), Dokki, P.O. 12622, Giza, Egypt*

Received 28 June 2020; accepted 11 October 2020
Available online 22 October 2020

KEYWORDS

Renewable biomass resources;
Cellulose;
Antibacterial activities;
Drug release

Abstract Pharmaceutical and clinicians researchers are looking for novel drug carriers to maintain the drug level in the body in low and effective dose. Thus, the present research concerned with studying the behavior of some natural biomass materials, namely microcrystalline cellulose, MCC, nanocrystalline cellulose, NCC, nanomethylcellulose, MC, and carboxymethyl cellulose, CMC, as a drug carrier materials for the Gentamicin sulphate, GM, by following up their rate of releasing the loaded drug with the time. Knowing of the initial rate of the releasing to each one and the sustaining rate along the period of the treatment, helps in choosing the best carrier for the drug that matches the patients requirements either whom are in need for a rapid dose (high level) of the drug followed by slow (low level) dose or those in need to start with the low level of the drug followed by high level of the drug. We chose MCC, NCC, MC and CMC, as natural, nontoxic biodegradable and renewable biomass materials, beside their low cost, to carry out this study. The results of the drug release, which measured by UV spectra, showed that the MCC, NCC, MC and CMC loaded with 0.025 g of the GM drug released 27.2%, 42.1%, 29.7%, 28.5% of the drug, respectively, along 10 days. All of them achieved the slow of the drug release but their behavior were different, where MCC, NCC and CMC started with low release then increased, and inversely, MC gave high rate of drug release and then decreased. The cause of this behavior was concerned to the adsorbing of the drug particles on the surface of the biomass materials or absorbing of the drug particles into the pores of the biomass materials. This was indicated by the study of their morphological image using the SEM, as well as indicating the presence of the functional group using the FT-IR study. The XRD, EDX and Agar Diffusion Assay, i.e. antimicrobial activity, against *Staphylococcus aureus, Escherichia Coli, Pseudomonas aeruginosa and Bacillus subtilis* were carried

* Corresponding author.
E-mail address: wkzawawy@yahoo.com (W.K. El-Zawawy).
Peer review under responsibility of King Saud University.

Production and hosting by Elsevier

https://doi.org/10.1016/j.arabjc.2020.10.018

out to make help in choosing of the best carrier convenient to the case of the illness requirement.

1. Introduction

Pharmaceutical and clinicians researchers are looking for novel drug carriers' technology forming drug delivery system that realize more targeting, sustaining therapeutic effects with little or without drug side effects on the patients′ body, especially those catch serious diseases, hypersensitivity and old ages. Drug delivery system is very important since it reaches the drug in a controlled manner (time period and releasing rate), maintains drug level in the body within therapeutic window and decreases the side effects of the drug by decreasing the drug dose. Bajpai et al. (2008) said that the targeted of the drug delivery is directed the drug towards a specific organ or tissue. Knowing of the level of the concentration of the drug at the beginning of the administration results in, constantly, changing the systemic drug concentrations in the body. This often produces a sharp initial increase in drug concentration to the level above the therapeutic range and followed by fast decrease in drug concentration below the therapeutic range. So, it is worthy restricting the best carriers through knowing of the concentration level of the drug at the beginning of the administration and the drug releasing rate of this carrier.

Schmaljohann (2006) reported that, drug delivery systems, DDS, often use polymeric carriers that act as "drug transporters". Using of it, as a carrier, allows to overcome of some problems appeared with the recent drugs development and application. Available polymeric based drug delivery system can be classified into four categories: Solvent-Activated Systems, Chemically Controlled Systems, Diffusion-Controlled Systems, and Magnetically Controlled Systems. Nair and Laurencin (2007) said that, biodegradable polymers are attractive for application in DDS since they do not require removal or additional manipulation. They can be easily metabolized and removed from the body. Since cellulose acetate, CA, electrospun nanofibers is a well biocompatible and biodegradable substrate to be applied in DDSs, Khoshnevisan, et al. (2018), has discussed incorporation of therapeutic agents of antibacterial, antiviral, anti-inflammatory agent, antineoplastic drugs, antioxidants, and also Ag-nanoparticles (NPs) into electrospun CA sheet, mat and nanofibers where it can be used as a carrier for therapeutic agents in drug delivery systems. Also, Yang, et al. (2020) incorporated ZIF-8 (zeolitic imidazolate framework-8) as a metal organic framework material into a laser-sintered PLLA (poly-L-lactic acid) scaffold which causes an improvement in the tensile and compressive strength by 36.9% and 85.6%, respectively. The releasing nutrient Zn element during the degradation enhances the cell adhesion, growth and differentiation which gives it great recommendation to use for bone repair.

On the other hand, many systems of the drug delivery systems were prepared but still the natural system is the best due to its safety. Sannino, et al. (2009) said that, utilization of agricultural waste is a pioneering and cellulose which isolated from agriculture wastes or chemically modified can be used in the biomedical applications as drug delivery system and wound dressing. Klemm, et al. (1998) reported that, cellulose has a unique chemical structure, which gives it a superior platform for several new biomaterials. Rowe, et al. (2006) mentioned that, cellulose and their derivatives have a long history as pharmaceutical excipients in various types of formulations. Li, et al. (2018) mentioned that, nanocellulose have gained more attention for antibacterial application due to their remarkable, special surface chemistry, physical properties, also for excellent biological properties. Nanocellulose can form nanocellulose-based antimicrobial materials when combine with polymers have antibacterial activities These polymers either natural polymers (chitosan and amino acid…) or synthetic polymers, (halogenated amines and guanidine salts,…). Nano crystalline cellulose(NCC)/chitosan (natural polymers) showed excellent antimicrobial activities against *Salmonella typhimurium* and *B. cereus*. Also, Poonguzhal, et al. (2017) pointed out that nano crystalline cellulose (NCC)/chitosan/poly (vinyl pyrrolidone) composites showed good blood compatibility and antimicrobial properties against *S. aureus* and *P. aeruginosa*.

Moreover, many researchers reported that nanocellulose with different materials can show great potential in biomedical applications, where they appeared to show a good effect against antibacterial and antifungal standard strains of *S. aureus*, *E. coli*, *C. albicans*and *A. niger* (Li et al., 2018, Lenselink and Andriessen, 2011, Jebali et al., 2013, Xu et al., 2013, Shao et al., 2017, Fortunati et al., 2012, Feese, et al., 2011, Jafary et al., 2015, Lefatshe et al., 2017, Shuai et al., 2020a, b). Furthermore, Yu-Ning, et al. (2020) prepared a multi-nanofibers composite film based on hybridization of bacterial cellulose nanofibers on chitin nanofibers (BCNF/CNF) and then precipitate Curcumin (Cur) which isolated from turmeric (natural material) as microspheres or nanoparticles in situ (BCNF/CNF) networks to form Cur/ BCNF/CNF smart film. The Cur/BCNF/CNF film showed excellent antibacterial activity against *S. aureus* and *E. coli* than the original BCNF film, he return this to the combination effect of Cur and CNF. Both CNF and Cur are coming from natural materials.

In the present study, since Egypt is an agriculture country and has a huge amount of agricultural wastes that producing after harvesting the crops, their cellulosic content can be successfully used in many field, pulp and paper, fiber board, pharmaceutical, cosmetic, medicine, textile, and food manufacture (Abou-Baker et al., 2019). Thus, cellulose was isolated from rice straw, as available agricultural wastes in Egypt, and was converted into microcrystalline cellulose, MCC, nanocrystalline cellulose, NCC, carboxymethyl cellulose, CMC, and methyl cellulose, MC, then used as drug loaded materials with Gentamicin sulphate.

Gentamicin was used where it belongs to a class of drugs known as aminoglycoside antibiotics. It is soluble in water (50 mg/ml), partially insoluble in alcohol and other organic solvents. Gentamicin is active against a wide range of bacterial infections (bactericidal), mostly Gram-negative bacteria including *Pseudomonas aeruginosa, Proteus mirabilis, Escherichia coli, Klebsiella pneumoniae, Enterobacter aerogenes, Serratia marcescens*, and the Gram-positive *Staphylococcus aureus*. It is used in the treatment of serious bone and joint infections caused by susceptible *Staphylococcus aureus, Citrobacter*

freundii, Enterobacter aerogenes, Escherichia coli, Klebsiella pneumoniae, Proteus mirabilis, Serratia marcescens, or *Pseudomonas aeruginosa*.

The current study was focused on the rate of the releasing of the drug a long 10 days to know the behavior of each of them through releasing of the drug and the drug′ concentration at the beginning of the release and interpret the cause of this behavior. As mentioned above knowing of the concentration of the drug at the beginning time of the drug administration is very important for serious hypersensitivity and the old adult patients. Morphological structure, FT-IR, XRD, EDX, UV spectra and Agar Diffusion Assay (antimicrobial activity) against *Staphylococcus aureus*, *Escherichia coli* (gram + ve), *Pseudomonas aeruginosa* and *Bacillus subtilis* (gram-ve) were carried out in NRC-Giza, Egypt and City of Scientific Research and Applied Technology, Alexandria, Egypt. *Staphylococcus aureus* and *Escherichia coli*, which were used in this study, are modified strains by the Genetic Engineering and Biotechnology Research Institute, City of Scientific Research and Applied Technology, Alexandria, Egypt.

2. Experimental

2.1. Materials

Agriculture residue, i.e. rice straw (Rs), was used as an available lignocellulosic material in Egypt and at the same time as a natural promising cellulosic source (Kim et al., 2004; Park et al., 2003; Sun and Gong, 2001). This lignocellulosic material can form pure cellulose after pulping and bleaching processes.

Gentamicin sulfate, GM, was provided from Science Lab. Com, INC, USA, and used in this study as the drug material**.** Monocholoroacetic acid was obtained from Aldrich Chemical Company Inc. (Milwaukee WI, USA), and sodium hydroxide, sodium chlorite, ethanol, methanol, acetone, and acetic acid, were used as received without further purification for the preparation of cellulose derivatives.

2.2. Compositional analysis of the agricultural waste

The lignocellulosic material was air dried, homogenized in separator and stored in polyethylene bags. The raw material was ground to a fine particle size before characterization. The agricultural waste should be ground to pass a 0.4-mm screen according to TAPPI T257 sp-12 (2012).

The moisture content, lignin and ash content of the raw material samples were determined according to TAPPI T264 cm-07 (2007), TAPPI T222 om-11 (2011), TAPPI T211 om-16 (2016), respectively.

For bleached pulped fiber sample, lignin and ash contents were determined as mentioned above, as well as α-cellulose which was estimated according to TAPPI T203 cm-09 (2009).

3. Methods

3.1. Cellulose isolation

Unbleached cellulose was isolated from Rs by a three steps pulping process, namely water-acid-alkali, as described in a previous work (El-Zawawy et al., 2011; Ibrahim et al., 2013). After that, bleached process was carried out by treating the unbleached cellulose fibers with sodium chlorite solution acidified with acetic acid for 1.5 h at 80 °C and liquor to fiber ratio was 10:1.5 this step was repeated for 3 times. The bleached cellulosic fibers were washed till neutrality and left to dry in air then stored for further use (Ibrahim et al., 2013; Wise and Karl, 1962).

3.2. Preparation of MCC

A mixture of sulfuric acid and bleached fibers (1 g of the fiber and 10 mL of 20% sulfuric acid) was placed in a round-bottom flask and placed in shaking water bath at 120° C. After heating for ø h, the mixture was cooled under −4° C, then neutralized with sodium carbonate. The powder was obtained by centrifugation, washed with distilled water until neutral pH and finally with acetone then air dried.

3.3. Preparation of NCC

As in case of the preparation of MCC, NCC was prepared by increasing the ratio between the bleached pulp and sulfuric acid to be 1:15 as well as increasing the time of the reaction that carried out at 120° C. At the end of the reaction time, the mixture was subjected to the homogenizer for 10 min followed by further 10 min treatment under sonication by using the ultrasound instrument SONICS VIBRA CELL. At the end, the powder was obtained by centrifugation, washed with distilled water until neutral pH and finally with acetone then air dried.

3.4. Preparation of nano-methyl cellulose

Methylation was carried out for NCC, where NCC was first mercerized at room temperature with 50% (w/v) NaOH in a liquor ratio of 1:10 (fiber : NaOH solution) for an hour. At the end of the time, the excess of NaOH was removed by filtration and 9 mL of acetone, as solvent, was added to the mercerized NCC. 3 mL of dimethyl sulfate was added dropwise, using separating funnel, to the mixture and the reaction was carried out at 50 °C for one hour. The addition of further dimethyl sulfate to the reaction mixture was repeated three times and in each time the reaction was proceeds for an hour. At the end, the reaction mixture was neutralized with 10% (v/v) acetic acid, filtered then washed with distilled water for three times followed by acetone, then dried at 50 °C under vacuum for 6 h.

3.5. Preparation of tosylated cellulose

Activation of the cellulosic material was carried out in which 10 g of the cellulosic material was first stirred in 18% (w/v) aqueous sodium hydroxide (200 mL) at room temperature for 6 h. The solution was filtered in G3 sintered glass and washed with distilled water for 6 times then twice with 100 mL dimethyl acetamide (DMAc).

The resulting cellulose was activated in 100 mL DMAc solution overnight. The solution was transferred in a 3 nicked flask and further 400 mL of DMAc was added and stirred for 2 h at 120 °C under reflux. At the end of the time, the temperature was down to 50 °C and 35 g of previously dried lithium chloride (LiCl) was added and stirring was continued for 24 h at room temperature till complete dissolution (Rahn et al., 1996).

Solution of 17.5 g tosylchloride in 25.0 mL triethylamine was added drop wise to the dissolved mixture with stirring for 24 h. At the end of the reaction time, precipitation was carried out in ice water with vigorously stirring. The precipitate was filtered in G3 funnel crucible, washed for 6 times with distilled water then with ethanol for further 6 times. Finally, the excess ethanol was removed by distillation and the precipitated was dried in a vacuum oven at 40 °C (Ibrahim et al., 2015).

3.6. Preparation of CMC

Carboxymethylation was carried out as follows: 5 g of air-dried tosylated cellulose (from rice straw) in 150 mL isopropanol was stirred vigorously, while 20.0 mL of 15% (w/v) aqueous NaOH was added dropwise during 10 min at room temperature. Stirring was continued for 1 h and 6 g of sodium monochloroacetate was then added. The mixture was placed on a water bath at 55 °C for 5 h with stirring. The mixture was filtrated, suspended in 300 mL of aqueous methanol and neutralized with acetic acid. The product was washed three times with 300 mL of 80% (v/v) aqueous ethanol and subsequently with 300 mL of 95% ethanol and dried in a vacuum oven at 60 °C (Heinze and Pfeiffer, 1999).

3.7. Drug loading

Antibiotic, Gentamicin Sulfate (GM) was loaded into MCC, NCC, CMC and MC, in which 0.025 g of GM dissolved in 1 mL of sterilized water was immersed with sterilized MCC, NCC, CMC and MC in a presence of sterilized water in a liquor ratio of 1:15 (fiber : water) and 15.0 mL of ethanol. The samples were incubated in a shaking incubator at 37° C for 72 h in order to assure complete absorption or desorption of the antibiotic with MCC, NCC, CMC and MC. The samples were then left to dry at room temperature for 24 h (Abd-Elhalem et al., 2020) and the total weight of the loaded samples were calculated as the weight of the sample plus the weight of the drug.

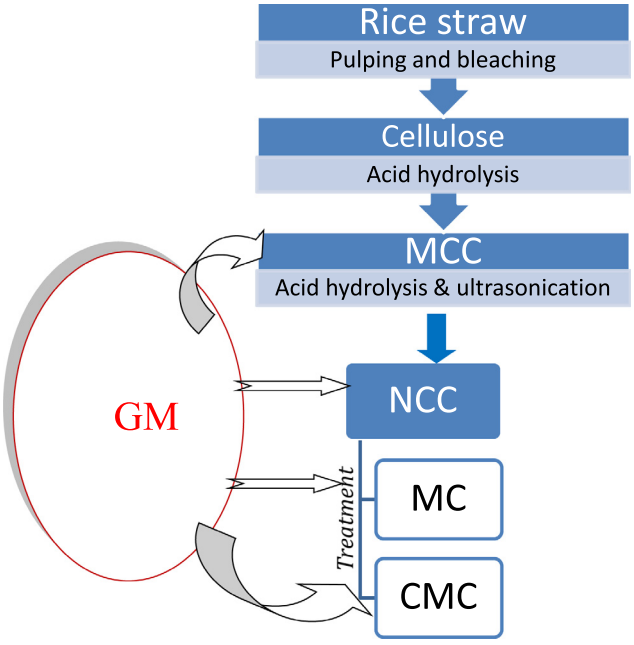

Flowchart for the experimental design

3.8. Characterization of the samples before and after drug loading

3.8.1. Scanning electron microscopy (SEM)

SEM was used to investigate the morphology of different samples, i.e. MCC, NCC, CMC and MC as well as the drug loaded samples, respectively, by using a scanning electron microscopy JEOL JXA-840A electron microprobe analyzer (JOEL USA Inc, Peabody, MA). The specimens were coated with gold/palladium and observed using an applied tension of 15.0 kV at a different magnifications.

3.8.2. FTIR spectroscopy

FT-IR spectroscopy was used for all the samples, with and without drug loaded. The IR spectra were performed using JASCO FT/IR 6100 Instrument. Samples (~2 mg) were mixed and thoroughly ground with ~ 200 mg KBr (Bociek and Welti, 1975). All the spectra were recorded in the absorbance mode from 4000 to 400 cm^{-1}.

From the FT-IR, the crystallinity index for the cellulosic samples resulting from rice straw can be calculated by two methods. The first one depends on the absorbance ratio from bands at 1376 cm^{-1} (A_{1376}) and 2916 cm^{-1} (A_{2916}), which known as Cr_1,

$$Cr\ Rs_1 = (A_{1376})/(A_{2916}) \quad (1)$$

while, the second one depends on the absorbance ratio from 1429 cm^{-1} (A_{1429}) and 897 cm^{-1} (A_{897}), which known as Cr_2.

$$Cr\ Rs_2 = (\ A_{1429})/(\ A_{897}) \quad (2)$$

where, bands of 2916 cm^{-1} and 897 cm^{-1} are assigned to the amorphous absorption bands, while the absorption band of 1429 cm^{-1} and 1376 cm^{-1} are known as the crystalline bands.

3.8.3. X-ray diffractometry (X-ray)

X-ray diffractometry patterns were recorded on Bruker D8 Advance X-ray diffractometer (Germany). The diffraction patterns were recorded using a secondary monochromator at 45 kV and 30 mA. The diffraction intensities were measured for Bragg angles (2Θ) in the range 10–50°. The crystallinity index was calculated according to Segal et al. (1959) and He et al. (2007).

3.8.4. Drug release measurements (In vitro)

In-vitro release of GM was carried out in phosphate-buffered saline solution (PBS, pH 7.4) at 37 °C, where,

First; Cellulose-gentamicin fibers (10 mg accurately weighted) were placed in dialysis cells containing 2 mL PBS. The tubes were incubated at 37° C. At each time point, the receiver compartment was collected and replaced with fresh PBS with the same volume.

Second; GM concentration was determined in each sample using UV-V Spectrophotometer (Cary 100 UV–Vis) at wavelength 232 nm.

3.9. Antibacterial assay

3.9.1. Antibiotic and strains used

Gentamicin sulphate was used as antibiotic for antibacterial assay against *Escherichia coli (E. coli)*, *Pseudomonas aerugi-*

nosa (P. aeruginosa), Bacillus subtilis (B. subtilis) and *Staphylococcus aureus (S. aureus)*. All of the models bacteria used were supplemented from Genetic Engineering and Biotechnology Research Institute, City of Scientific Research and Technological Application, Alexandria, and maintained on Luria–Bertani media (LB) g/l (peptone 10, yeast extract 5, sodium chloride 5 and agar 20) solid agar medium at 4 °C until used.

3.9.2. Assay of antibacterial activity

The antibacterial activity of the GM-cellulose derivatives were investigated by disc and agar well technique (Alagumaruthanayagam et al., 2009; Bajpai et al., 2013) against *E. coli* and *P. aeruginosa* as as Gram-negative model bacteria and *B. subtilis* and *S. aureus* as Gram-positive model bacteria. The antibacterial activity effect of the undiluted samples were evaluated by the disc (piece) diffusion technique (25 mg/ piece) and those diluted samples by the agar well diffusion technique (0.5 cm of well diameter). For both techniques, the samples were plased (piece) or each well contain 75 µl from diluted samples on *E. coli*, *P. aeruginosa, S. aureus* and *B. subtilis* cultured spread (optical density at 660 nm reached 0.2) on agar plates (one piece or well per plate). Each one of the cellulose derivatives was used as a control. The agar plates were then incubated at 37 °C for 48 h and the antibacterial activity of samples were photographed and determined by measuring the diameter of inhibition zone and compared with their control. Triplicate experiments were done for each sample (Luan et al., 2012; Subtaweesin et al., 2018).

4. Results and discussion

The lignocellulosic material, i.e. Rs, was chemically analysed as a raw material and after pulping and bleaching processes, for holocellulose, lignin and ash content. It was shown that the lignin content decreased after pulping from 14.30% to 2.10% and reached to 0.01% after bleaching process. The holocellulose of the raw material was 69.5%, while the α-cellulose after pulping was 76.30%, and the hemicellulose was 16.6%. After bleaching processes, α-cellulose was increased to 98.2%, and the ash content decreased from 16.0% to 0.05%, while the yield was decreased from 76.1% to 56.3%.

The FTIR spectroscopic analysis of the bleached rice straw pulp is shown in Fig. 1a. The broad band at 3401 cm^{-1} represents stretching vibration of –OH group of cellulose, while that at 2916 cm^{-1} characterized the –CH stretching vibration of cellulose. The peak at 1705 cm^{-1}, which is attributed either to the acetyl and uronic ester groups of the hemicelluloses or to the ester linkage of carboxylic group of the ferulic and p-coumeric acids of lignin and/or hemicelluloses does not appeared in the FTIR spectra for rice straw bleached pulp, this indicates the removal of most of the hemicelluloses and lignin from the fibers during the bleaching process. The absorption band at 1631 cm^{-1} represents the C-O of the glycosidic unit of cellulose. The peaks at 1429 cm^{-1} and that at 1376 cm^{-1} in the spectrum represent bending vibration of C-H (scissoring motion in cellulose). Disappearance of the peak at 1537 cm^{-1}, Fig. 1a, which represents C = C of aromatic ring of lignin in the rice straw bleached pulp, indicates the removal of lignin during the bleaching process. The lack of bands at 1705 cm^{-1} and at 1537 cm^{-1}, Fig. 1a, indicate the removal

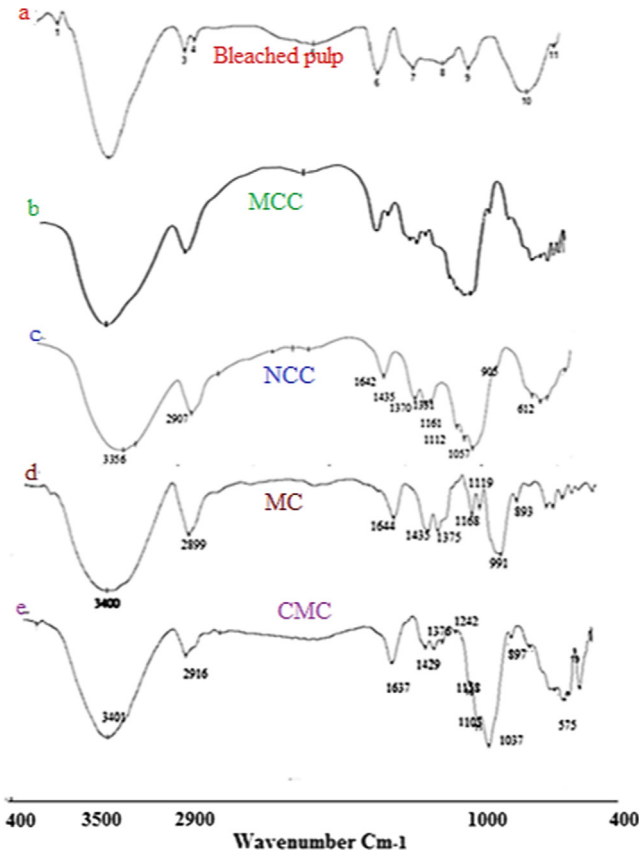

Fig. 1 FT-IR for: (a) bleached Rs; (b) MCC; (c) NCC; (d) NMC and (e) Tosyl-CMC.

of lignin and hemicelluloses in the rice straw bleached pulp. The absorption band at 1242 cm^{-1} represents out of plane bending vibration of C-OH at C6. The bands at 1165 cm^{-1} and 1158 cm^{-1} represent C-C ring stretching vibration, while band at 1103 cm^{-1} characterized the stretching vibration of the ether linkage (1,4-D glycoside) of cellulose. On the other hand, the absorption bands at 1033 cm^{-1} and 1037 cm^{-1} represent C-O-C and C-O-H stretching vibration of ether groups at pyranose ring in cellulose, while absorption band at 897 cm^{-1} is assigned to C-O-C stretching vibration at β-(1 → 4) glycosidic linkage. Moreover, the crystallinity of the resulting cellulosic material for bleached rice straw pulp was calculated from FT-IR and was found to be 0.832.

On the other hand, MCC and NCC prepared from the bleached pulp of rice straw was characterized by FT-IR. The results recorded that, IR spectral peacks are broader and sharper in the NCC due to more hydrogen bonding in it, as shown in Figure (1c). Also, we can notice the absence of the two bands related to lignin and hemicellulose at 1750 cm^{-1} and 1560 cm^{-1}. The strong broad band characteristic to O-H streching vibration was shifted to lower wavenumber from 3400 cm^{-1} to 3356 cm^{-1} for both MCC and NCC, Figure (1b&c).

The absorption bands at 2899 cm^{-1} and 2907 cm^{-1}, which correspond to C-H stretching vibration, are shown to be broader, stronger and shifted towards lower wavenumber values with increasing in their intenisities indicating the decrease in the amorphouse region, where those peaks are known as

amorphouse bands. This means increasing in the crystallinity of MCC and NCC samples. Also, the broad and strong band at 1435 cm^{-1} shows an increase in its intensity indicating the increase in the degree of crystallinity of both MCC and NCC samples, where this band is known as the crystallinity band. Moreover, the bands at 1375 cm^{-1} and 1370 cm^{-1}, which are known as crystallinity bands, appeare as broad, strong and sharp with increasing in their intensities meaning an increase in the crystallinity of the MCC and NCC samples. While, the absorption band at 893 cm^{-1}, in the MCC sample, which is assigned to C-O-C streching vibrtion of β(1–4)-glycosidic linkage, is known as the amorphouse band of the sample indicating the presence of amorphouse part in this sample. The apperance of a very weak band at 905 cm^{-1} in the NCC, Figure (1c), with very low intensity indicates the presence of amorphouse part in a tiny amount. This conferms the increase in the crystallinity part in the NCC.

The ratio of the crystallinity was calculated from FT-IR as described in the experimental part by two methods, i.e. Cr_1 and Cr_2. From the two equations, 1 and 2, it was observed that for MCC, Cr_1 was 0.77 and Cr_2 was 1.16, while for NCC, the Cr_1 was 0.86 and Cr_2 was 1.91.

Furthernore, The FTIR for MC was studied and shown in Fig. 1d. The stretching vibration of O-H group was recognized from the absorption band at 3442 cm^{-1}, while the symmetrical stretching vibration band for C-H group was shown at 2917 cm^{-1}. The peack at 1422 cm^{-1} represents bending vibration of CH, while the peaks at 1376 cm^{-1} , 1320 cm^{-1} and 896 cm^{-1} represent the C-H stretching vibration of CH_2 and CH_3 and that at 1109 cm^{-1} represents the C-O-C stretching vibration of β-(1–4) glycosidic linkage (Rimdust et al., 2012; Maity et al., 2012; Nadaur et al., 2017).

Moreover, in this work, CMC was prepred from the tosylated NCC. Fig. 1e shows that, absorption band at 3433 cm^{-1} was appeared broader and stronger, so as the absorption band at 2921 cm^{-1} for C-H stretching vibration appears as stronger and broader. The absorption bands at 1636 cm^{-1}, 1445 cm^{-1} and 1410 cm^{-1} are assigned to COO^-

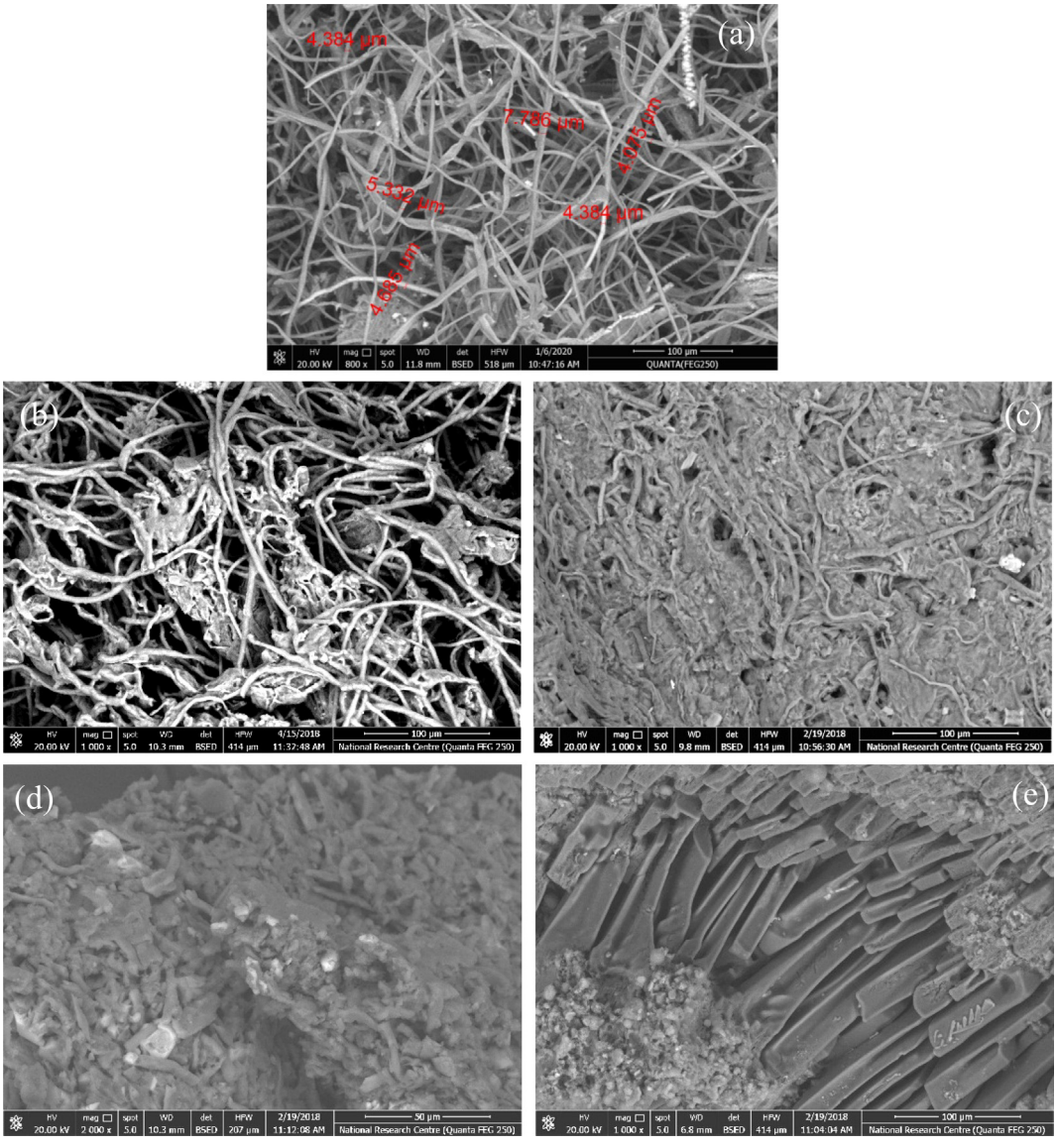

Fig. 2 SEM for: (a) bleached rice straw pulp (800x); (b) MCC (1000x); (c)NCC (1000x); (d) NMC (2000x); and (e) CMC (1000x).

asymmetric and symmetric stretching vibration of carboxylic group, CH bending vibration for methyl group and S = O stretching vibration for sulfonyl chloride. Absortion bands at 1376 cm^{-1} and 1327 cm^{-1} were assigned to CH stretching vibration of CH_2 and CH_3 group. The band at 1110 cm^{-1} was assigned to C-O-C stertching vibration, while absorption bands at 1044 cm^{-1} and 1024 cm^{-1} were assigned to S-O and C-O groups, respectively, and that at 898 cm^{-1} was assigned to β(1–4) glycosidic linkage that confirms the presence of both carboxyl and tosyl groups on the cellulose unites.

Morphological structure for the bleached pulp rice straw, as well as MCC, NCC, MC and CMC were detected using SEM and seen in Fig. 2. The SEM image shows that the fibers of the bleached rice straw, Fig. 2a, appeared as individual fibers. On the other hand, the study of the SEM cleared that both the MCC and NCC appeared as thin fibers, but NCC appeared thiner than that of the MCC, Fig. 2b&c. For MC, the morphological structure appeared like a tiny particles agglomerated together to form small particles like rod shape, while for nano-CMC it appeared in the form of soft and small particles which gathered together and form a rod shape.

The XRD has been the most widely used technique to investigate structures through measuring of the crystallinity index (CrI) and crystallinity size (CrS) (I_{200}) of cellulose and cellulose based materials. Since NCC is the starting material for our study after being prepared from the cellulose isolated from Rs to be used for the preparation of both MC and CMC, so the XRD for NCC was studied and illustrated in Fig. 3. It showed four peaks at 2Θ of 7° which refers to amorphous region, while peaks at 15.3°, 22.2° and 34.6° characterized to the cellulose structure. The peak at 22.2°, with high intinisty, is characterized to the crystallinity region. The CrI of NCC was 83.0%, and the CrS was 0.58. When cellulose undergoes an acid hydrolysis treatment, the impurities and most of the amorphous regions are removed and the majority of the crystalline parts remain (Santmartí and Lee, 2018). Moreover, the alkali and acid treatments convert part of the crystalline structur from cellulose I to cellulose II. XRD of MCC shows that the CrI was 70% and the CrS was 0.69. The results confirmed that NCC is more crystalline than MCCand has smaller crystal size which makes it with more surface area than MCC.

4.1. Drug delivery system formation

Many researches were concerned with using the natural biomass materials in the formation of the drug delivery system due to their safety and biodegradability beside they do not require removal or additional manipulation and they can be easily metabolized and removed from the body. MCC, MC and CMC were widely used as pharmaceutical excipients or as a tablet matrix-former material or film forming material (Katikaneni et al., 1995; Upadrashta et al., 1994; Siepmann et al., 2007). CMC is used not only as emulsifier, gel-former, but also as binding agent or disintegrates in tableting (Chen et al., 2010; Wan and Prasad, 1989).

In this study, we used the cellulose which was isolated from the agricultural residues, i.e. rice straw, for the preparation of different cellulose derivatives, i.e. MCC, NCC, MC and CMC. They were used, by us, in the biomedical application by loading them with GM, which is used as an inflammation antibiotics drug. GM was loaded to all the cellulosic derivatives to form fusion drug release system. The drug was loaded physically into each one of those products and the releasing of the drug was measured as function of the time.

4.1.1. Drug loading (fusion drug release system)

As mentioned, the cellulose derivatives, i.e. MCC, NCC, MC and CMC, which are known as nontoxic natural polymers, biodegradable, compatible, renewable and sustainable materials, were loaded with GM in a ratio of 0.2 g/0.025 g to form Fusion Drug Release System. EDX, SEM, FT-IR and UV spectrophotometer were studied to identify the presence of the drug into the materials since GM includes both N and S in its chemical structure, $C_{60}H_{125}N_{15}O_{25}S$, and to measure its released concentration as a function of the time. From this study, the behaviour of each cellulosic derivative after loading the drug and the path way through which the drug exits can be known.

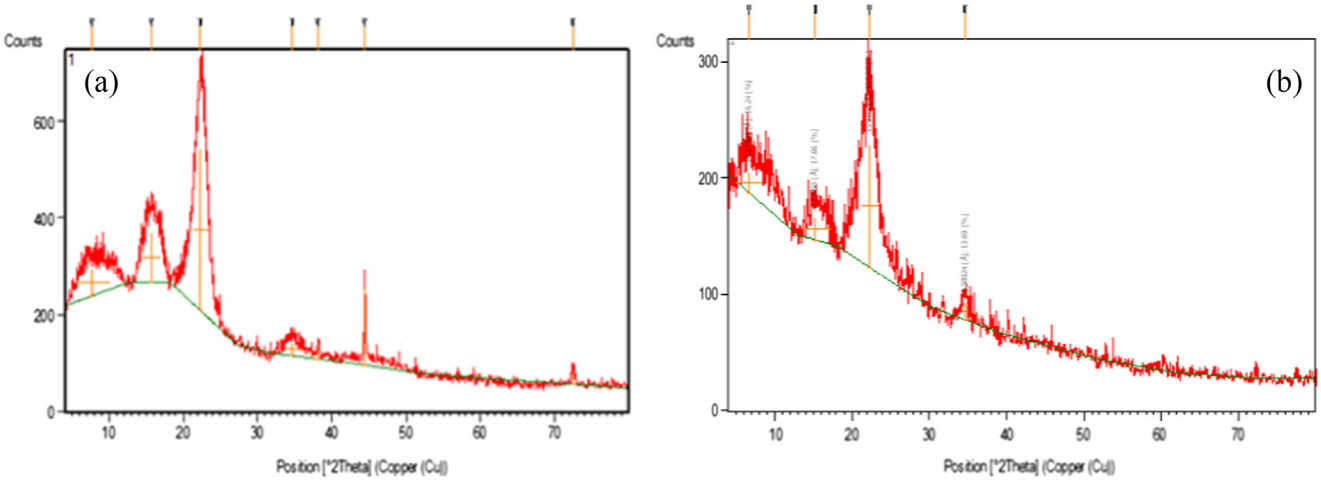

Fig. 3 The XRD of: (a) MCC and (b) NCC.

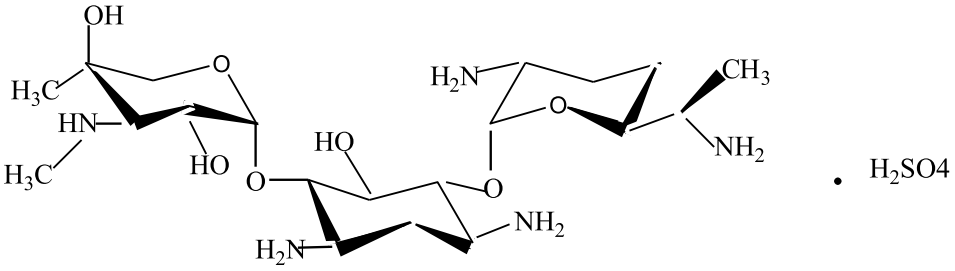

Chemical Structure of Gentamicin Sulfate

EDX was carried out for all the samples that were loaded with the drug and the results were shown in Fig. 4 and gathered in Table1.The presence of the drug was confirmed by the presence of N and S element which belong to GM in all the samples. This proves that the cellulosic materials were loaded by the drug.

4.2. FT-IR spectra after loading the drug

The FT-IR spectra was used to confirm the loading of the drug, where the FT-IR for the drug alone and for the samples after loading the drug were detected and shown in Fig. 5. In Fig. 5, the FT-IR spectra confirms the presence of GM that was loaded into MCC, NCC, CMC and MC, where the same groups that belongs to the GM, shown in circules, were appeared in all the loaded samples. In another word, the peaks which belong to GM at 3530 cm^{-1}, 3471 cm^{-1}, 3300 cm^{-1} and 3205 cm^{-1}, that represent the bending vibrations of –NH and –OH, and those appeared at 1587 cm^{-1}, 1269 cm^{-1}, 1079 cm^{-1}, 1033 cm^{-1} and 899 cm^{-1}, which are characterized to NH and SO groups, and the absorption band at 1585 cm^{-1}, that represents the C = N, are all appeared in the FT-IR for the loaded samples of MCC, NCC, MC and CMC, with either little shift of the peaks or broader pands to the peaks, stronger or sharper. This proves that the loading of the GM was done either by adsorption on the surface of the samples or by absorption inside thier pores.

4.2.1. Drug release

As mentioned in the experimental part, the antibiotic drug (GM) was loaded onto the samples MCC, NCC, MC and CMC, and the drug realse was studied, where it is known as the amount of the drug that was released out from the sample in a measured time, and this was carried out using UV spectrophtometer. The results that were gathered in the Table 2 showed that, after 30 min the MC followed by NCC gave high values from the concentration of the drug that was released, i.e. $3.86x10^{-3}$ and $1.00x10^{-3}$, respectively, while MCC and CMC gave low values for the drug released, i.e. $6.71x10^{-4}$ and $4.8x10^{-4}$, respectively. This means that the particles of the drug which adsorbed on the surface of the MC, and NCC are more than that adsorbed on the surface of the MCC and CMC, where adsorption means that the drug particels are loosly bouned on the sample surface and thus made them more easier to release and move to the media solution. This was confirmed by the SEM for the drug loaded samples, Fig. 6, where the SEM was carried out to prove whether the particles of the drug were absorbed into the pores of the fibers or adsorbed onto the surface of the fibers. Fig. 6A-D illustrated the presence of the drug on the surface of the nanofibers, i.e. adsorbed, as well as some of them were impregnated into the fibers pores, i.e. absorbed. Also, from the SEM we can see the difference between MC and CMC, in which most of the drug was adsorbed on the surface of MC while some of it was adsorbed onto the surface of CMC and the others were shown to be inside the fibers. This contributed as an important factor in the drug release since the drug paricels which adsorbed onto the surface of the MC are loosly bounded through hydrogen bonding that occurred between both the MC and GM, so, the durg particles can be easly released at the first minutes while the particels of the drug that were inside the MC pores takes a time to be released. On the other hand, the reason that makes the behavior of CMC looks different is due to that the CMC is a water soluble derivative, so it turns to gel-form or emulsifier form, which gives the drug particels time to release from the CMC and when the water diffuses indide CMC it helps the drug particels to release easier causing higher rate for the drug release. Also, the presence of COO^- group, i.e. caboxylic groups, may form a cloud of negative charge around the CMC fibers that acts as a berrier to prevent the entering of the drug particels into the CMC fibers leading them to be adsorbed on the surface and thus released easily. Moreover, the SEM for the MCC shows that the drug particels were both adsorbed on the surface, as seen by the red arrow, and absorbed inside the fibers, as seen in the blue circule. The slow realse in case of the MCC can be due to the presence of the drug inside the fibers more than being at the surface.

Furthermore, the SEM image for NCC shows a great adsorbed particels of the drug on the surface of the NCC fibers which lead to the increase of the initial release of the drug. Also, MC has a great paticels of the durg on its surface (adsorbed) which causes the increase of the initial releasing rate of the drug.

Table 2 and Fig. 7 cleared that MCC released about 27.2%, while MC and CMC released 29.7% and 28.5%, respectively. Thus, it can be noticed that MCC is the slowest one in the drug release followed by CMC and MC. This indicates that MCC is the best drug release material, since they release approximately the same rate along 10 days followed by NCC.

Since all of the materials under investigation are natural and non toxic and are used in the food industries as addatives or thikners, thus, this encourage the researchers to use them in

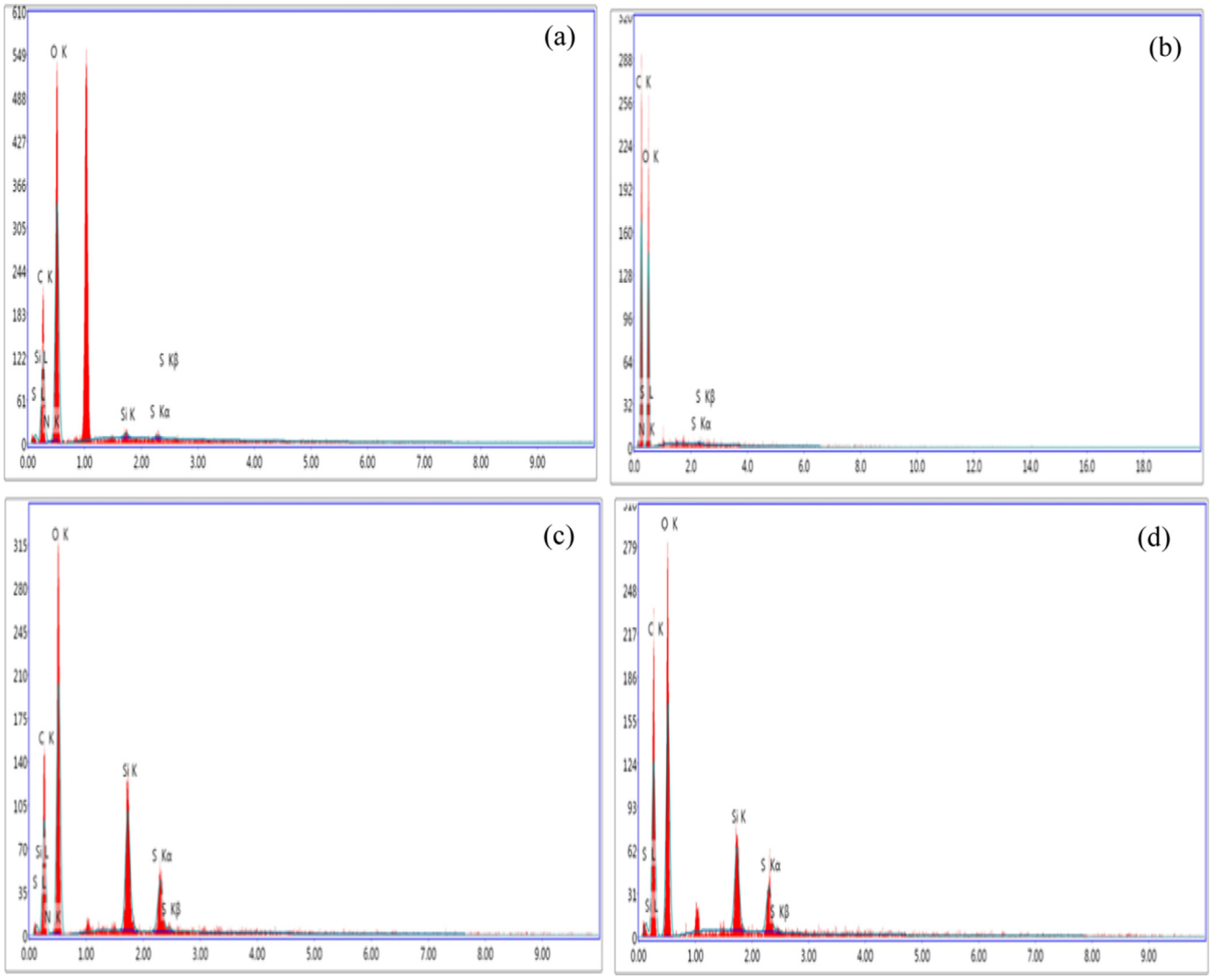

Fig. 4 EDX of (a) NCC-GM, (b) MCC-GM, (c) CMC-GM and (d) MC-GM.

Table 1 EDX for dug loaded samples.

Sample	Element (wt%)				
	C	O	Si	N	S
MCC with GM	48.25	51.14	0,61	0.49	0.21
NCC with GM	32.24	66.66	0.36	0.48	0.26
CMC with GM	37.51	53.44	5.61	0.58	2.86
MC with GM	44.24	49.61	2.59	0.23	2.33

the medicine field. For GM drug, both MCC and NCC are the best to be used for their slow and maintenance release. The slow starting and then maintenance performance is more useful since GM causes hypersensitivity, or kidenys problems, or increase pressure inside the skull especialy in the older adults. While MC is the best with the sever and serious bacterial infections.

From the above results, it can be noticed that the celluolsic derivatives can be divided according to their release rate into: 1st starts releasing of the drug slowly, and then begin with slow rate and making maintenance for the drug release over a long period, like MCC, and 2nd starts with increasing in the rate of the drug release then begin to decrease making slow release and maintenance of the drug release rate, like NCC. 3rd starts with an initial rapid and high releasing of the drug followed by a slow release and then recorded high increasing of the drug release rate followed by decreasing in the rate of the drug release and then making maintenance in the rate of drug

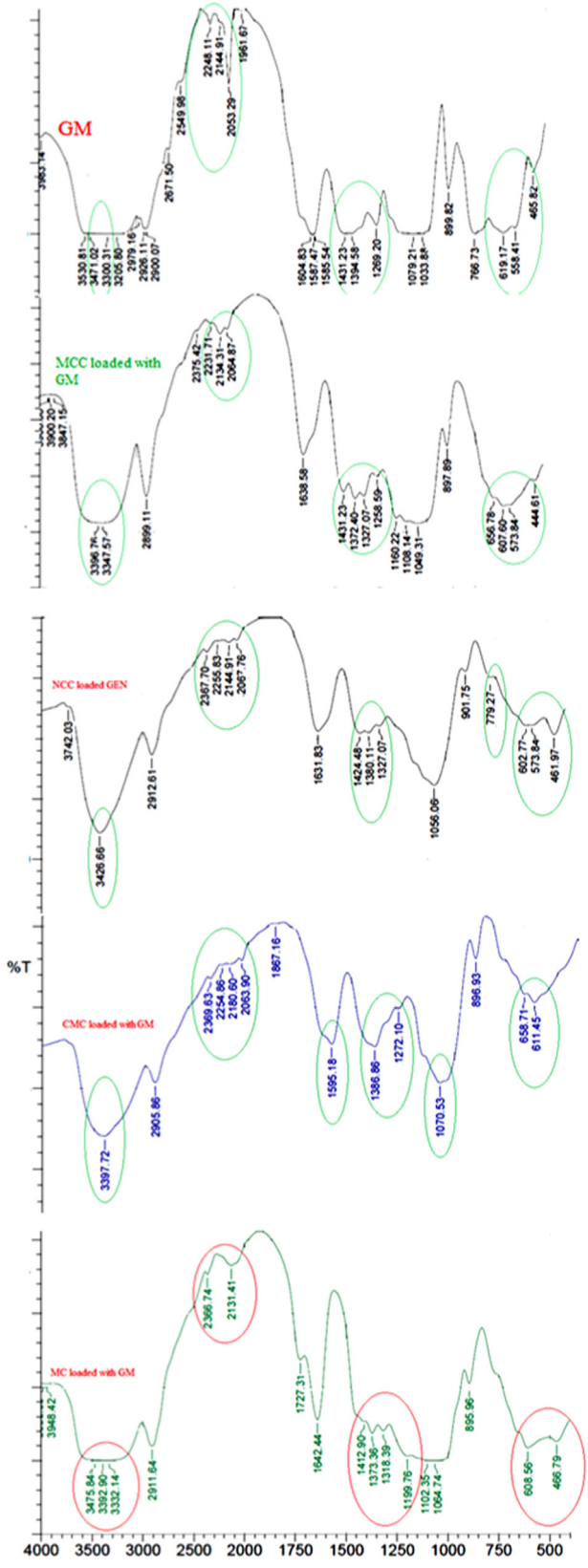

Fig. 5 FT-IR spectra for GM alone, MCC, NCC, CMC and MC loaded with GM samples.

release, like MC. 4th starts with increasing in the drug release rate followed by decreasing in the drug release rate then begin to give high increase in the drug release rate followed by decreasing approximately at the same rate of increasing then begin a slow release till reaches maintenance state, like CMC. All of them can be divided into two categories; one starts with releasing of the drug slowly and achieves the maintenance rate of the drug release, like MCC, NCC and CMC, The other category starts with rapid and high releasing of the drug, like MC. Both of them are acceptable, because some of the illness need to start with high level of the dose, followed by slow release which is more important in the sever and serious bacterial infection, while the others need the inverse, with realizing the maintenance to decrease the amount of the dose of the drug that enters the body′s patients to avoid some side effects like hypersensitivity, that caused by the drug, and also nerve disease and, sometimes, increasing pressure inside the skull, where the dose is usually taken 4 times over 24 h based on the patients′ pretreatment body weight for 7–10 days.

Generally, fusion drug release system initially releases either high or low portion of the dose to attain rapidly the effective therapeutic concentration of the drug. Then, drug release kinetics follow a well defined behavior to realize the maintenance dose to enable the attainment of the desired drug concentration. This means that each system presents its own advantages as well as limitations.

4.2.2. Antibacterial assay

GM is an aminoglycoside molecule used as bactericidal against a broad spectrum of microorganisms and issued in clinical applications as the treatment of infected skin cysts, ulcers, burns, infected insect bites and stings, infected lacerations, and wounds (Gubernator et al., 2007; Kovács et al., 2012). Various studies reported that the GM as antibiotic model was loaded on different composites such as, cotton cellulose/polyacrylic (CC/PAAc) composite loaded by GM and used the mixture as antibacterial against *E. coli* (Bajpai et al., 2013), polydopamine nanoparticles loaded with GM and tested against *S. aureus* and *P. aeruginosa* (Batul et al., 2020), $CaCO_3$ nanoparticles (CCNPs) as carriers of GM and used as antibacterial against *B. subtilis* (Pan et al., 2018).

The antibacterial activaty of the loaded GM-Cellulose derivatives were detected and compared to GM as a control using Gram-positive and negative bacteria. The antibacterial activity effect of the antibiotic alone was evaluated by the disc (piece) diffusion technique and those loaded on different cellulose derivatives by the agar well diffusion technique. In order to assess this antibacterial activity, the inhibtion zones of bacterial growth were measured for all the samples. Four different cases, i.e. A, B, C and D, were studied, in which the case A referred to the all samples were used without any dilutions, while the casses B, C and D, referred to the diluted samples for 0.5:1, 1:1 and 25:1 (mg /mL), respectively. The results were gathered in Table 3 and Fig. 8 (case A only).

The antibacterial activities against Gram-negative bacteria were studied. In case A, the drug loaded samples of MCC, MC and CMC showed an inhibition zone diameter of 0.86,

Table 2 Drug release for MCC, NCC, MC and CMC loaded GM samples.

	Sample			
Time	MCC	NCC	MC	CMC
30 min	6.71×10^{-4}	1.00×10^{-3}	3.86×10^{-3}	4.8×10^{-4}
24 h	1.06×10^{-3}	2.45×10^{-3}	1.15×10^{-3}	1.77×10^{-3}
48 h	9.50×10^{-4}	1.94×10^{-3}	9.73×10^{-4}	1.58×10^{-3}
72 h	9.42×10^{-4}	1.60×10^{-3}	6.22×10^{-4}	7.73×10^{-3}
96 h	7.88×10^{-4}	1.21×10^{-3}	2.64×10^{-3}	8.10×10^{-4}
168 h	7.21×10^{-4}	8.8×10^{-4}	5.50×10^{-4}	6.30×10^{-4}
192 h	6.17×10^{-4}	7.69×10^{-4}	3.92×10^{-4}	2.35×10^{-4}
216 h	5.43×10^{-4}	6.70×10^{-4}	4.20×10^{-4}	3.84×10^{-4}
240 h	5.05×10^{-4}	4.73×10^{-4}	$2.90 \times \times 10^{-4}$	4.29×10^{-4}
$\sum$ C	6.8×10^{-3}	10.5×10^{-3}	7.4×10^{-3}	7.1×10^{-3}
% Drug release	27.2	42.1	29.7	28.5

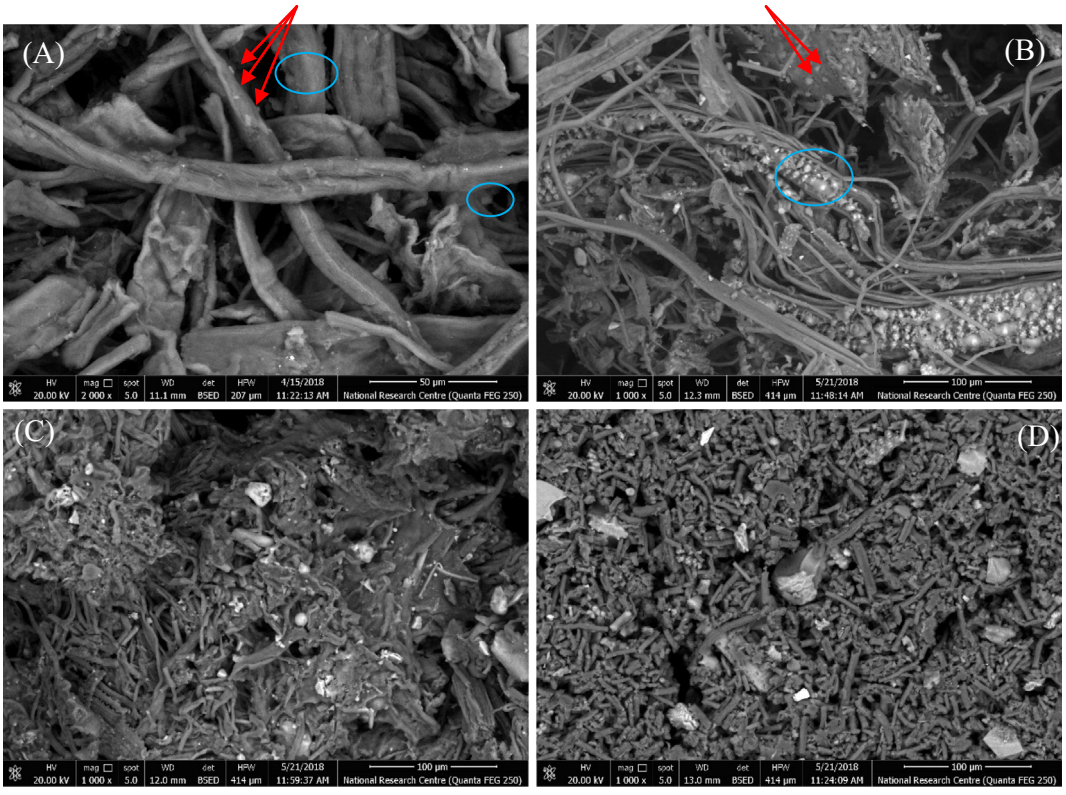

Fig. 6 SEM for drug loaded samples; (A) MCC-GM, (B) NCC-GM, (C) MC-GM and (D) CMC-GM.

0.56 and 0.083 cm. For cases B, C and D they show a zero results, i.e. they show inactive antibacterial activity against *E. coli* compared with the GM alone that shows an inhiition zone diameter of 1.3 cm.

The antibacterial activities against *P. aeruginosa* was also studied for the drug loaded samples and compared with the drug itself. The results that were gathered in Table 3 show that drug loaded samples with CMC, MCC and MC gave equal or lower inhibition zone diameter compared with GM alone. The CMC, MCC and MC gave inhibition zone of 2.4, 1.7 and 1.4 cm compared with 2.4 cm for GM alone in case A, while in case (B) the inhibition zone increased for the antibacterial activity against the *P. aeruginosa* with CMC, 3.1 cm, and MCC, 2.5 cm, compared with GM alone (2.3 cm). For MC, it exhibited inactive antibacterial activity against the *P. aeruginosa*. This could be due to the role of the water, where CMC and MCC absorbe water and a swelling occurs so the drug can be easily released and thus affects the strain which led to increase in the antibacterial activity against the *P. aeruginosa*. This enterpretion agreed with the results in the case of MC which changed from inactive, i.e. 0 cm in the inhibition zone to 1.8 cm. NCC approximately exhibited the same antibacterial activity against *P. aeruginosa*, i.e. 2.5, 2.4 and 2.3 cm, respectively. For case D, all the values of the antibacterial activities against the *P. aeruginosa* were increased, i.e. CMC (3.5 cm), MCC (2.6 cm), MC (2.0 cm) and NCC (1.4 cm). Case D appeared to be the best results and this may be referred to the increase of the drug to 25 mg.

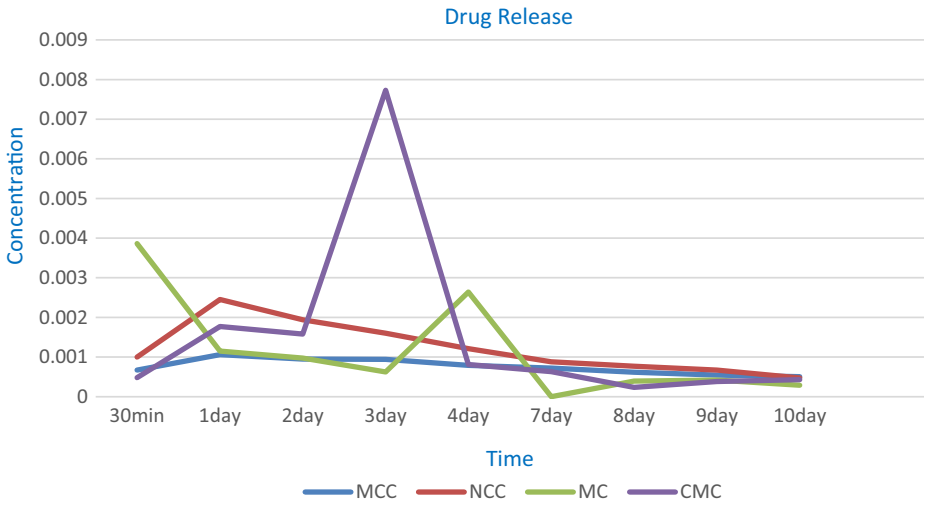

Fig. 7 Drug release for MCC, NCC, MC and CMC loaded GM samples.

Table 3 Inhibition zone diameters (cm) of all cases using MCC, NCC, CMC, MC and GM samples against *E. coli*, *P. aeruginosa*, *B. subtilis* and *S. aureus*.

Bacteria	Samples	Diameter of inhibition zones (cm)			
		Cases			
		A	B	C	D
E. Coli	MCC	0.86 ± 0.01	0	0	0
	NCC	0 ± 0.01	0	0	0
	CMC	0.83 ± 0.02	0	0	0
	MC	0.56 ± 0.01	0	0	0
	GM	1.3 ± 0.0	0	0	0
P. aeruginosa	MCC	1.7 ± 0.01	2.5 ± 0.02	0	2.6 ± 0.04
	NCC	0 ± 0.003	0	2.4 ± 0.02	1.4 ± 0.01
	CMC	2.4 ± 0.01	3.1 ± 0.1	0	3.5 ± 0.01
	MC	1.4 ± 0.01	0	1.8 ± 0.04	2.0 ± 0.04
	GM	2.4 ± 0.0	2.3 ± 0.1	0	0
B. subtilis	MCC	3.6 ± 0.03	2.4 ± 0.0	0	4.1 ± 0.02
	NCC	1.4 ± 0.02	0	1.9 ± 0.03	2.2 ± 0.01
	CMC	0	3.1 ± 0.2	0	3.8 ± 0.07
	MC	3.9 ± 0.2	0	0	1.7 ± 0.0
	GM	2.6 ± 0.1	3.6 ± 0.1	0	0
S. aureus	MCC	2.2 ± 0.0	0	0	0
	NCC	0	0	0	0
	CMC	1.1 ± 0.01	0	0	0
	MC	0	0	0	0
	GM	0.60 ± 0.01	0	0	2.4 ± 0.03

Case (A): the sampleloaded the drug without any dilution.
Case (B): the sample loaded the drug as 1 mg/1mL dist. water.
Case (C): the sample loaded the drug as 0.5 mg/1mL dist. water.
Case (D) the sample loaded the drug as 25 mg/1mL dist. water.

On the other hand, the effects of all the samples against Gram-positive bacteria were studied. In case A, the drug loaded with CMC gave higher antibacterial activities against the *B. subtilis* compared with GM alone, where it gave inhibition zone of 3.9 cm, for CMC, compared with 3.7 cm, for GM alone, while MCC gave inhibition zone of 3.6 cm, i.e. it approached to that of using GM alone. For MC it gave lower inhibition zone compared with GM alone against the *B. subtilis*, where it gave 1.4 cm. In case B, all the values of the antibacterial activities against the *B. subtilis* gave lower inhibition zone compared with that of the GM alone except for CMC which gave 3.1 cm, and only drug loaded with MC has no antibacterial activity against the *B. subtilis*. In case C, NCC gave lower inhibition zone, i.e. 1.9 cm and MC still has no effect against the *B. subtilis*. For case D, the best results were given with MCC (4.1 cm), and using MC showed an increase in the inhibition zone to reach 1.7 cm compared to that 1.4 cm when used in case A. Also, NCC gave higher values

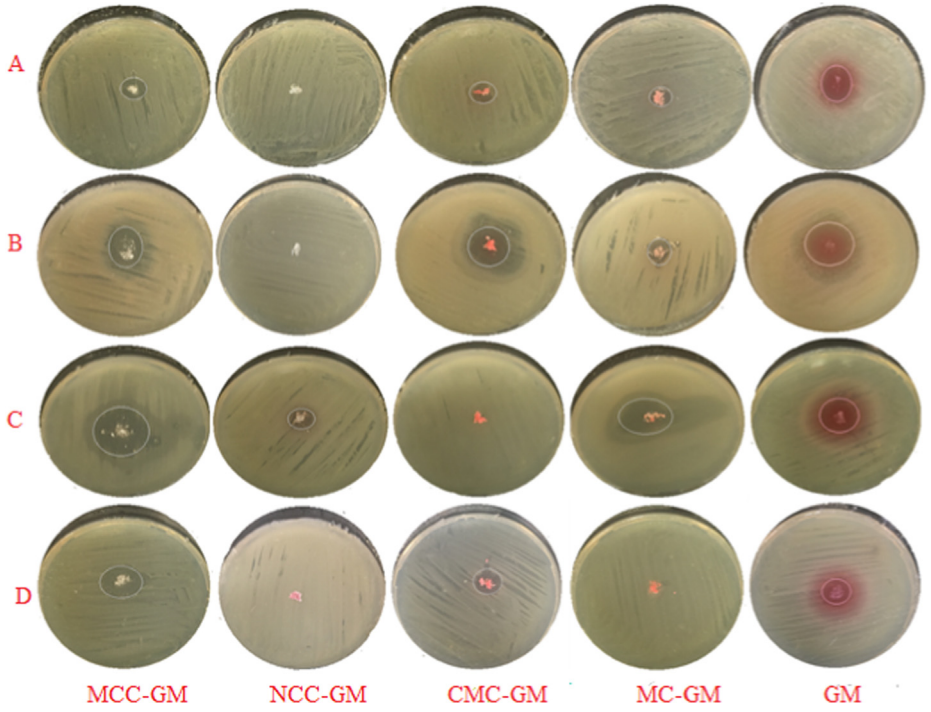

Fig. 8 Optical images of inhibition zones diameter of case A only using MCC, NCC, CMC, MC and GM samples against **(A)** *E. coli*, **(B)** *P. aeruginosa*, **(C)** *B.subtilis* and **(D)** *S.aureus*.

when used in case D compared with those in case C. For case A, the inhibition zone diameter of 2.2 and 1.1 cm for drug loaded samples of MCC and CMC showed a great increase in the antibacterial activities against the *S. aureus* compared to GM alone (0.60 cm), while they gave zero results, i.e. show no antibacterial activities, in both cases B and C.

In general, the disk and well diffusion results showed that the cellulosic derivatives (fibers)-GM and free GM have a more marked antibacterial effect against the model used Gram positive bacteria than on the Gram negative bacteria. It is evident that the outer membrane of the Gram negative bacteria most probably acts as an extra barrier to the antibacterial effects of the GM. Gram positive bacteria lack this outer membrane that may explain their greater sensitivity. We can conclude that the antibacterial action resulting from undiluted samples (case A) becomes more effective with greater area of inhibition zone than diluted samples (cases B, C and D).

5. Conclusions

One of the challenges in pharmaceutical study is to choose the best natural materials that release the minimum dose for completing the cure. By knowing the material behavior during the releasing of the drug we can determine the best loading material for the drug especially for serious, hypersensitivity and the old aged patients.Our study indicated that the selected natural materials, i.e. MCC, NCC, MC and CMC can all be divided into two categories as drug carriers. The first category is the one that started with releasing the drug slowly and achieving the maintenance rate of the drug release, like MCC, NCC and CMC which are conventional to the patients who suffered from hypersensitivity toward GM and the elderly. The other category is the one that started with the rapid and high release of the drug, like MC which can be used in the serious diseases. From this study we can conclude that both NCC and MCC are the best to be used for GM because of their slow release. Moreover, the decreased and increased behavior in the drug release rate with CMC and MC may be referred to the presence of the carboxylic and methyl groups. On the other hand, the agar diffusion results showed that the cellulosic-gentamicin fibers and free gentamicin have a substantially clearer antibcterial effect against the gram-positive bacterium, *B. subtilis*, than on the gram-negative bacteria, *P. aeruginosa* and *E. coli*. We can conclude that the antibacterial action resulting from undiluted samples, case A, becomes more effective with greater area of inhibition zone than diluted samples, cases B, C and D.

Acknowledgment

The authors would like to acknowledge Dr. Ahmed Saleh Kherah, Researcher at Cellulose and Paper Department, National Research Centre, for carrying out the antibacterial assay and the discussion for its data.

References

Abd-Elhalem, S.S., El-Shinnawy, N.A., Abu-El Magd, E.E., El Zawawy, W.K., Haggag, N.Z., 2020. Application of either nano fibrillated cellulose methotrexate or nano silicon dioxide methotrexate composites against renal fibrosis in leukemia rat model. Int. J. Biol. Macromol. 157, 329–339.

Abou–Baker, N. H., Ouis, M., Abd–Eladl, M., and Ibrahim, M. M. (2019). "Transformation of Lignocellulosic Biomass to Cellulose–Based Hydrogel and Agriglass to Improve Beans Yield," Waste and Biomass Valorization,Published online 16 May 2019. Doi: 10.1007/s12649-019-00699-6.

Alagumaruthanayagam, A., Pavankumar, A.R., Vasanthamallika, T. K., Sankaran, K., 2009. "Evaluation of solid (disc diffusion)-and liquid (turbidity)-phaseantibiogram methods for clinical isolates of diarrheagenic*E. coli* and correlation with efflux". The Journal of antibiotics. 62 (7), 377–384.

Bajpai, K., Shukla, S.K., Bhanu, S., Kankane, S., 2008. Responsive polymers in controlled drug delivery. Prog. Polym. Sci. 33 (11), 1088–1118.

Bajpai, S., Das, P., Sharma, L., 2013. Investigation of dynamic release of antibiotic drug gentamicin sulphate from cotton cellulose/polyacrylic acid composite fibers. J. Macromolecular Sci. Part A 50 (1), 55–64.

Batul, R., Bhave, M.J., Mahon, P., Yu, A., 2020. Polydopamine nanosphere with in-situ loaded gentamicin and its antimicrobial activity. Molecules 25 (9), 2090.

Bociek, S.M., Welti, D., 1975. The quantitative analysis of uronic acid polymers by infrared Spectroscopy. Carbohydr. Res. 42, 217–226.

Chen, R.N., Ho, H.O., Yu, C.Y., Sheu, M.T., 2010. Development of swelling/floating gastroretentive drug delivery system based on a combination of hydroxyethyl cellulose and sodium carboxymethyl cellulose for Losartan and its clinical relevancein healthy volunteers with CYP2C9 polymorphism. Eur. J. Pharm. Sci. 39 (1–3), 82–89.

El-Zawawy, W.K., Ibrahim, M.M., Abdel-Fattah, Y.R., Soliman, N. A., Mahmoud, M.M., 2011. Acid and enzyme hydrolysis to convert pretreated lignocellulosic materials into glucose for ethanol production. Carbohydr. Polym. 84, 865–871.

Feese, E., Sadeghifar, H., Gracz, H.S., Argyopoulos, D.S., Ghiladi, R. A., 2011. PhotobacterialPorphyrin–cellulosenanocrystals: synthesis, characterization and antimicrobial properties. Biomacromolecules 12 (10), 3528–3539.

Fortunati, E., Armentano, I., Zhou, Q., Iannoni, A., Saino, E., Visai, L., Berglund, L.A., Kenny, J.M., 2012. Multifunctional bionanocomposite films of poly(lactic acid), cellulose nanocrystals and silver nanoparticles. Carbohydr. Polym. 87 (2), 1596–1605.

Gubernator, J., Drulis-Kawa, Z., Dorotkiewicz-Jach, A., Doroszkiewicz, W., Kozubek, A., 2007. In vitro antimicrobial activity of liposomes containing ciprofloxacin, meropenem and gentamicin against gram-negative clinical bacterial strains. Lett. Drug Des. Discovery 4 (4), 297–304.

He, J., Tang, Y., Wang, S.Y., 2007. Differences in morphological characteristics of bamboo fibers and other natural cellulose fibers: studies on X-ray diffraction, solid state 13C-CP/MAS NMR, and second derivative FTIR spectroscopy data. Iran. Polym. J. 16, 807–818.

Heinze, T., Pfeiffer, K., 1999. Studies on the synthesis and characterization of carboxymethylcellulose. Die AngewandteMakromolekulareChemie. 266, 37–45.

Ibrahim, M.M., El-Zawawy, W.K., Jüttke, Y., Koschella, A., Heinze, T., 2013. Cellulose and microcrystalline cellulose from rice straw and banana plant waste: preparation and characterization. Cellulose 20, 2403–2416.

Ibrahim, M. M., Fahmy, T. Y. A., Salaheldin, E. I., Mobarak, F., Youssef, M. A., and Mabrook, M. R. (2015)."Synthesis of tosylated and trimethylsilylated methyl cellulose as pH- Sensitive carrier matrix," Life Science Journal. 12(1), 29-37.

Jafary, R., Mehrizi, M.K., Hekmatimoghaddam, S.H., Jebali, A., 2015. Antibacterial property of cellulose fabric finished by allicin-conjugated nanocellulose. J. The Textile Institute. 106 (7), 683–689.

Jebali, A., Hekmatimoghaddam, S., Behzadi, A., Rezapor, I., Mohammadi, B. H.,Jasemizad, T., Yasini, S. A., Javadzadeh, M., Amiri, A., Soltani, M., Rezaei, Z., Sedighi, N., Seyfi, M., Rezaei, M., Sayadi, M. (2013). "Antimicrobial activity of nanocelluloseconjugatedwithallicin and lysozyme," Cellulose. 20, 2897–2907.

Katikaneni, P.R., Upadrashta, S.M., Neau, S.H., Mitra, A.K., 1995. Ethylcellulose matrix controlled release tablets of a water-soluble drug. Int. J. Pharm. 123 (1), 119–125.

Khoshnevisan, K., Maleki, H., Samadian, H., Shahsavari, S., Sarrafzadeh, M.H., Larijani, B., Dorkoosh, F.A., Haghpanah, V., Khorramizadeh, 2018. Cellulose acetate electrospunnanofibers for drug delivery systems: applications and recent advances. Carbohydr. Polym. 198, 131–141.

Kim, H. S., Yang, H. S., Kim, H. J., and Park, H. J. (2004). "Thermogravimetric analysis of rice husk flour filled thermoplastic polymer composites," .Journal of Thermal Analysis and Calorimetry. 79, 395–404.

Klemm, D., Philipp, B., Heinze, T., Heinze, U., and Wagenknecht, W. (1998). In: "Comprehensive Cellulose Chemistry: Fundamentals and Analytical Methods," Volume 1, Wiley-VCH Verlag GmbH.

Kovács, E., Savopol, T., Iordache, M.-M., Săplăcan, L., Sobaru, I., Istrate, C., et al, 2012. Interaction of gentamicin polycation with model and cell membranes. Bioelectrochemistry 87, 230–235.

Lefatshe, K., Muiva, C.M., Kebaabetswe, L.P., 2017. Extraction of nanocellulose and in-situ casting of ZnO/cellulose nanocomposite-with enhanced photocatalytic and antibacterial activity. Carbohydr. Polym. 164, 301–308.

Lenselink, E., Andriessen, A., 2011. A cohort study on the efficacy of a polyhexanide-containing biocellulose dressing in the treatment of biofilms in wounds. J. Wound Care. 20 (11), 536–539.

Li, J., Cha, R., Mou, K., Zhao, X., Long, K., Luo, H., Zhou, F., Jiang, X., 2018. Nanocellulose-Based Antibacterial Materials. Adv. Healthcare Materials. 7, 1800334.

Luan, J., Wu, J., Zheng, Y., Song, W., Wang, G., Guo, J., Ding, X., 2012. Impregnation of silver sulfadiazine into bacterial cellulose for antimicrobial and biocompatible wound dressing. Biomed. Mater. 7 (6), 11.

Maity, D., Mollick, M.M., Mondal, D., Bhowmick, B., Bain, M.K., Bankura, K., 2012. Synthesis of methyl cellulose.Silvernanocomposite and investigation of mechanical and antimicrobial properties. Carbohydr. Polym. 90 (4), 1818–1825.

Nadaur, M., Boukraa, F., Quradi, A., Benaboura, A., 2017. Effects of methyl cellulose on the properties and morphology of polysulfone membranes repared by phase inversion. Mater. Res., 10

Nair, L.S., Laurencin, C.T., 2007. Biodegradable polymers as biomaterials. Prog. Polym. Sci. 32, 762–798.

Pan, X., Chen, S., Li, D., Rao, W., Zheng, Y., Yang, Z., et al, 2018. The synergistic antibacterial mechanism of gentamicin-loaded CaCO3 nanoparticles. Front. Chem. 5, 13.

Park, B.D., Wi, S.G., Lee, K.H., Singh, A.P., Yoon, T.H., Kim, Y.S., 2003. Characteriza-tion of anatomical features and silica distribution in rice husk using microscopic and micro-analytical techniques. Biomass Bioenergy 25, 319–327.

Poonguzhali, R., Basha, S.K., Kumari, V.S., 2017. Synthesis and characterization of Chitosan-PVP-nanocellulose composites for *in-vitro* wound dressing application. Int. J. Biol. Macromol. 105 (1), 111–120.

Rahn, K., Diamantoglou, M., Klemm, D., Berghmans, H., Heinze, T., 1996. Homogeneous synthesis of cellulose p-toluenesulfonates in N, N-dimethylacetamide/LiCl solvent system. Macromol. Mater. Eng. 238 (1), 143–163.

Rimdust, S., Somsaeg, K., Kewsuwan, P., Jubsilpc, C., Tiptiakorns, S., 2012. Comparison of gamma radiation crosslinking and chemical crosslinking on properties of methyl cellulose hydrogel. Eng. J. 16 (4), 15–28.

Rowe, R. C., Sheskey, P. J., and Owen, S. C. (2006). In: "Handbook of Pharmaceutical Excipients,"Washington, DC: American Pharmacists Association.

Sannino, A., Demitri, C., Madaghiele, M., 2009. Biodegradable cellulose-based hydrogels design and applications. *Materials* 2, 353–373. https://doi.org/10.3390/ma2020353.

Santmartí, A., and Lee, K-Y. (2018). "Crystallinity and Thermal Stability of Nano cellulose," In: Nanocellulose and Sustainability: Production, Properties, Applications, and Case Studies. Lee, K-Y. (Ed.), Taylor & Francis Group, LLC.

Schmaljohann, D., 2006. Thermo- and pH-responsive polymers in drug delivery. Adv. Drug Deliv. Rev. 58 (15), 1655–1670.

Segal, L., Greely, J.J., Martin, A.E., Conrad, C.M., 1959. An empirical method forestimating the degree of crystallinity of native cellulose using X-raydiffractometer. Text. Res. J. 29, 786–794.

Shao, W., Wu, J., Liu, H., Ye, S., Jiang, L., Liu, X., 2017. Novel bioactive surface functionalization of bacterial cellulose membrane. Carbohydr. Polym. 178, 270–276.

Shuai, C., Yuan, X., Yang, W., Peng, S., He, C., Feng, P., Qi, F., Wang, G., 2020a. Cellulose nanocrystals as biobased nucleation agents in poly-l-lactide scaffold: Crystallization behavior and mechanical properties. Polym. Test. 85 (106458), 1–10.

Shuai, C., Liu, G., Yang, Y., Qi, F., Peng, S., Yang, W., He, C., Wang, G., Qian, G., 2020b. A strawberry-like Ag-decorated barium titanate enhances piezoelectric and antibacterial activities of polymer scaffold. Nano Energy 74, 104825.

Siepmann, F., Hoffmann, A., Leclercq, B., Carlin, B., Siepmann, J., 2007. How to adjust desired drug release patterns from ethylcellulose-coated dosage forms. J. Control. Release 119 (2), 182–189.

Subtaweesin, C., Woraharn, W., Taokaew, S., Chiaoprakobkij, N., Sereemaspun, A., Phisalaphong, M., 2018. Characteristics of curcumin-loaded bacterial cellulose films and anticancer properties against malignant melanoma skin cancer cells. Appl. Sci. 8 (7), 1188–1202.

Sun, L., Gong, K., 2001. Silicon-based materials from rice husks and their applications. J. Indust. Eng. Chem. Res. 40, 5861–5877.

TAPPI T257 sp-12. (2012). "Screening of pulp (Somerville-type equipment)," TAPPI Press, Atlanta, GA.

TAPPI T264 cm-07. (2007). "Preparation of Wood For Chemical Analysis," TAPPI Press, Atlanta, GA.

TAPPI T222 om-11. (2011). "Acid-insoluble lignin in wood and pulp," TAPPI Press, Atlanta, GA.

TAPPI T211 om-16. (2016). "Ash in wood, pulp, paper and paperboard:combustion at 525°C," TAPPI Press, Atlanta, GA.

TAPPI T203 cm-09. (2009). "Alpha-, beta- and gamma-cellulose in pulp," TAPPI Press, Atlanta, GA.

Upadrashta, S.M., Katikaneni, P.R., Hileman, G.A., Neau, S.H., Rowlings, C.E., 1994. Compressibility and compactibility properties of ethylcellulose. Int. J. Pharm. 112 (2), 173–179.

Wan, L.S.C., Prasad, K.P.P., 1989. Uptake of water into tablets with low-substituted carboxymethyl cellulose sodium as disintegrant. Int. J. Pharm. 55 (2–3), 115–121.

Wise, E.L., Karl, H.L., 1962. Cellulose and hemicellulose. In: Libby, C.E. (Ed.), Pulp and paper science and technology. McGraw-Hill, New York.

Xu, W.Z., Gao, G., Kadla, J.F., 2013. Synthesis of antibacterial cellulose materials using a "clickable" quaternary ammonium compound. Cellulose 20, 1187–1199.

Yang, Y., Zan, J., Yang, W., Qi, F., He, C., Huang, S., Peng, S., Shuai, C., 2020. Metal organic frameworks as a compatible reinforcement in a biopolymer bone scaffold. Mater. Chem. Front. 4, 973–984.

Yu-Ning, Y., Kun-Ying, L., Wang, P., Yi-Cheng, H., Min-Lang, T., Fwu-Long, M., 2020. Development of bacterial cellulose/chitin multi-nanofibers based smart films containing natural active microspheres and nanoparticles formed *in situ*. Carbohydrate Polymer. 228, 115370.